Vorticity wave interaction, Krein collision, and exceptional points in shear flow instabilities

Cong Meng [1,2] and Zhibin Guo [2,*]
[1] *Southwestern Institute of Physics, P.O. Box 432, Chengdu 610041, China*
[2] *State Key Laboratory of Nuclear Physics and Technology, Fusion Simulation Center, School of Physics, Peking University, Beijing 100871, China*

(Received 31 March 2023; accepted 4 December 2023; published 28 December 2023)

We relate the model of vorticity wave interaction to Krein collision, $\mathcal{PT}$-symmetry breaking, and the formation of exceptional points in shear flow instabilities. We show that the dynamical system of coupled vorticity waves is a pseudo-Hermitian system with nonreciprocal coupling terms. Krein signatures of the eigenvalues are illustrated as the signs of the action of the vorticity waves. Interaction between positive-action and negative-action vorticity waves then corresponds to the Krein collision between eigenvalues with opposite Krein signatures, the spontaneous breaking of $\mathcal{PT}$ symmetry, and the formation of exceptional points. The control parameter of the $\mathcal{PT}$-symmetry-breaking bifurcation is the ratio between frequency detuning and coupling strength of the vorticity waves. The critical behavior near the exceptional points is described as a transition between phase-locking and phase-slip dynamics of the vorticity waves. The phase-slip dynamics correspond to nonmodal, transient growth of perturbations in the regime of unbroken $\mathcal{PT}$ symmetry, and the phase-slip frequency $\Omega \propto |k - k_c|^{1/2}$ shares the same critical exponent with the phase rigidity of system eigenvectors.

DOI: 10.1103/PhysRevE.108.065109

I. INTRODUCTION

The interaction of vorticity waves has been widely shown to be a physical interpretation of Kelvin-Helmholtz instabilities [1–6], and naturally provides a nonmodal approach to study optimal growth and transient dynamics in shear instabilities [7–9], as thoroughly reviewed in [10]. Instability requires that the dispersion relations of isolated vorticity waves intersect, and that the actions of the vorticity waves have opposite signs [10]. The mechanism of instability onset is interpreted as phase locking and mutual growth of counterpropagating vorticity waves. The model of coupled vorticity waves can be reframed into a minimal dynamical system [11,12], where the onset of shear instabilities corresponds to a bifurcation of fixed points from two neutral centers to a pair of stable and unstable nodes [11].

On the other hand, the role of symmetries and symmetry-breaking bifurcations in fluid dynamics has long been recognized [13,14], and it has recently come to light that Kelvin-Helmholtz instability is the result of spontaneous parity-time ($\mathcal{PT}$) symmetry breaking [15–17]. In the framework of spectral analysis of pseudo-Hermitian, or equivalently, G-Hamiltonian systems [18–22], the real eigenvalues can be classified into three kinds with Krein signatures ± 1 or 0. Krein collision refers to the process that two real eigenvalues with opposite Krein signatures collide and move off the real axis, and split into complex-conjugate pairs [18]. Kelvin-Helmholtz instability onset is then interpreted as the Krein collision between eigenvalues [23]. These results, however, have not yet been related to the mechanism of vorticity wave interaction.

In this work, we relate the model of vorticity wave interaction to the spectral analysis of Krein collision and $\mathcal{PT}$-symmetry breaking in shear flow instabilities. We show that the dynamical system of coupled vorticity waves is a pseudo-Hermitian system with nonreciprocal, non-Hermitian coupling terms. Isolated vorticity waves form the Hermitian component of the system and correspond one to one to the eigenmodes. Krein signatures of the eigenvalues are illustrated as the signs of the action of the corresponding vorticity waves. Phase-locking and mutual growth of counterpropagating vorticity waves then correspond to the Krein collision between eigenvalues with opposite Krein signatures, the spontaneous breaking of $\mathcal{PT}$ symmetry, and the formation of exceptional points. The control parameter of the $\mathcal{PT}$-symmetry-breaking bifurcation is shown to be the ratio between frequency detuning and coupling strength of the vorticity waves. The analysis of $\mathcal{PT}$-symmetry breaking in shear flow instabilities is thus closely related to other systems extensively studied in non-Hermitian optics or photonics, such as coupled cavities or waveguides [24,25].

The most striking feature of non-Hermitian systems is the existence of exceptional points (EPs) [14,24–26]. EPs are spectral singularities on the complex eigenvalue plane where both the real and imaginary parts of the eigenvalues are identical, and where the eigenvectors also coalesce. The eigenvectors are extremely nonorthogonal near an EP, so that when a system operates around the EP, it becomes highly sensitive to perturbations of the system [24–26]. The transient dynamics such as power oscillations and amplifications near the EP are actively investigated in the context of non-Hermitian optics and photonics [27–29]. In this work,

*zbguo@pku.edu.cn

we adopt the model of vorticity wave interaction to describe the critical behavior and transient dynamics near the EPs in shear flow instabilities. In particular, we demonstrate that the transition of phase dynamics from a phase-slip state to a phase-locking state [30,31] corresponds to the spontaneous breaking of $\mathcal{PT}$ symmetry across the EP. The phase-slip dynamics near the EP are highly nonuniform in time and lead to nonmodal, transient growth of perturbations [32–35] in the regime of unbroken $\mathcal{PT}$ symmetry. The phase-slip frequency $\Omega \propto |k-k_c|^{1/2}$ shares the same critical exponent with the phase rigidity of eigenvectors, which measures the nonorthogonality of system eigenvectors near the EP.

This work is organized as follows. In Sec. II, we review the model of vorticity wave interaction and recast the model into a pseudo-Hermitian dynamical system. In Sec. III, we relate the wave interaction mechanism to the stability theory of pseudo-Hermitian systems and demonstrate how the interaction between positive-action and negative-action vorticity waves corresponds to the Krein collision between eigenvalues with opposite Krein signatures. In Sec. IV, we adopt the model of vorticity wave interaction to explain the role of $\mathcal{PT}$-symmetry breaking and demonstrate the formation of EPs in shear flow instabilities, and describe the critical behavior and transient dynamics near the EPs. We summarize and discuss our results in Sec. V.

II. THE MODEL OF VORTICITY WAVE INTERACTION

A. The general model

Consider a two-dimensional, incompressible, and inviscid shear flow without density stratification, where the background state is a mean flow in the y direction with profile $U(x)$. The velocity field is $\boldsymbol{v}=(v_x,v_y)=(-\partial\phi/\partial y,\partial\phi/\partial x)$, where ϕ is the stream function, and the vorticity $\boldsymbol{q}=\nabla\times\boldsymbol{v}$ of a two-dimensional flow reduces to a scalar $q=\nabla^2\phi$. The vorticity equation reads $dq/dt=0$, where $d/dt=\partial/\partial t+\boldsymbol{v}\cdot\nabla$. To analyze the stability of the shear flow, denote perturbations of the background state as $v_x=\tilde{v}_x$, $v_y=U(x)+\tilde{v}_y$, $q=q_0+\tilde{q}$, and $\phi=\phi_0+\tilde{\phi}$, where the mean vorticity $q_0=\nabla^2\phi_0=U'$ and mean vorticity gradient $q_0'=\partial q_0/\partial x=U''$. (We use primes to denote ∂_x.) Then the linearized equation of perturbed vorticity is

$$\frac{\partial\tilde{q}}{\partial t}+U\frac{\partial\tilde{q}}{\partial y}=U''\frac{\partial\tilde{\phi}}{\partial y}. \tag{1}$$

Equation (1) expresses the generation of vorticity perturbations by the background mean vorticity gradient, in terms of the source term $U''\partial\tilde{\phi}/\partial y$. If all the perturbations are assumed to have normal mode form as $\tilde{\phi}(x,y,t)=\hat{\phi}(x)e^{ik(y-ct)}$ and $\tilde{q}(x,y,t)=\hat{q}(x)e^{ik(y-ct)}$, then the Rayleigh stability equation [10,36]

$$(U-c)(\hat{\phi}''-k^2\hat{\phi})=U''\hat{\phi} \tag{2}$$

is obtained for normal mode analysis of the problem.

In our work, we take the nonmodal approach [33,34] and keep the time-dependent form of perturbations $\tilde{\phi}(x,y,t)=\hat{\phi}(x,t)e^{iky}$ and $\tilde{q}(x,y,t)=\hat{q}(x,t)e^{iky}$, with Fourier transform in the y direction, assuming that all the perturbations are monochromatic with certain wave number k. Then the linearized initial value problem is

$$\tfrac{\partial\hat{q}}{\partial t}+ikU\hat{q}=ikU''\hat{\phi}, \tag{3a}$$

$$\hat{q}=\hat{\phi}''-k^2\hat{\phi}. \tag{3b}$$

We note that the assumption of monochromatic perturbations is adequate since any perturbations in general can be expressed as a linear superposition of perturbations with different wave numbers.

Equation (3b) is the Poisson equation and can be solved as

$$\hat{\phi}(x,t)=\int G(x,x')\hat{q}(x',t)dx', \tag{4}$$

where the Green function kernel $G(x,x')$ describes a nonlocal $\hat{\phi}-\hat{q}$ coupling [37]. For boundary conditions $\hat{\phi}(\pm\infty)=0$, the kernel is $G(x,x')=-e^{-k|x-x'|}/(2k)$.

For a discretized, piecewise profile of background shear layer, neutrally stable vorticity waves are induced on each interface of vorticity jump, and the direction of intrinsic propagation is determined by the sign of the vorticity gradient [10]. In general, consider a piecewise shear layer with n interfaces,

$$q_0'(x)=U''(x)=\sum_{j=1}^{n}\Delta\bar{q}_j\delta(x-x_j), \tag{5}$$

where $\Delta\bar{q}_j=q_0(x_j^+)-q_0(x_j^-)$ is the vorticity jump across the interface $x=x_j$. The vorticity perturbations thus vanish at all locations except at the interfaces, i.e.,

$$\hat{q}(x,t)=\sum_{j=1}^{n}q_j(t)\delta(x-x_j). \tag{6}$$

Note that we have ignored the continuous spectrum part of the solution where initial vorticity perturbations are passively advected by the background flow and remain stable [7]. Equation (4) is then translated into

$$\hat{\phi}(x,t)=-\frac{1}{2k}\sum_{j=1}^{n}q_j(t)e^{-k|x-x_j|}. \tag{7}$$

Let $q_j(t)=Q_j(t)e^{i\theta_j(t)}$, then Eq. (3a) can be written in amplitude-phase form,

$$\frac{dQ_i}{dt}=k\Delta\bar{q}_i\sum_{j\neq i}G_{ij}Q_j\sin\theta_{ij}, \tag{8a}$$

$$\frac{d\theta_i}{dt}=-\omega_i+k\Delta\bar{q}_i\sum_{j\neq i}G_{ij}\frac{Q_j}{Q_i}\cos\theta_{ij}, \tag{8b}$$

where $\theta_{ij}=\theta_i-\theta_j$ and $G_{ij}=-e^{-k|x_i-x_j|}/(2k)$. The frequency of each individual mode,

$$\omega_i=kU_i+\frac{\Delta\bar{q}_i}{2}, \tag{9}$$

includes both the intrinsic frequency $\Delta\bar{q}_i/2$ and the Doppler shift by the *in situ* shear flow U_i. Equation (9) tells that each single interface of background vorticity jump $\Delta\bar{q}_i$ induces a neutrally stable vorticity wave, and the direction of phase speed, $v_{ph}=\Delta\bar{q}_i/(2k)$, in the reference frame moving with U_i, is determined by the sign of the vorticity jump.

Equations (8a) and (8b) describes a dynamical system that models vorticity wave interaction in a general shear layer with multiple interfaces. The system has a canonical Hamiltonian representation in action-angle form [38,39], with the Hamiltonian

$$H=\sum_i \omega_i I_i-\frac{1}{2}\sum_{j\neq i} G_{ij}Q_iQ_j\cos\theta_{ij}=-\sum_i I_i\dot{\theta}_i, \quad (10)$$

where $I_i=Q_i^2/(2k\Delta\bar{q}_i)$ is the action of each vorticity wave. The canonical Hamiltonian equation follows as

$$\frac{\partial H}{\partial I_i}=-\dot{\theta}_i, \quad \frac{\partial H}{\partial \theta_i}=\dot{I}_i. \quad (11)$$

B. Dynamical system and linear operators

From a mathematical point of view, the stability of shear flows can be analyzed from the spectral theory of linear operators [14]. For the model of vorticity wave interaction, the dynamical system given by Eqs. (8a) and (8b) can be written in linear, complex form,

$$\dot{q}_i=-i\omega_i q_i-i\Delta\bar{q}_i\sum_{j\neq i}\sigma_{ij}q_j, \quad (12)$$

where $\sigma_{ij}=-kG_{ij}=e^{-k|x_i-x_j|}/2$ is the coupling strength between vorticity waves. The matrix form is then

$$\dot{\boldsymbol{q}}=\mathbf{A}\boldsymbol{q}, \quad \boldsymbol{q}=\begin{pmatrix} q_1\\ \vdots \\ q_n\end{pmatrix}, \quad (13)$$

where $\mathbf{A}=-i\mathbf{H}$, and the Hamiltonian operator is

$$\mathbf{H}=\begin{pmatrix} \omega_1 & \Delta\bar{q}_1\sigma_{12} & \cdots & \Delta\bar{q}_1\sigma_{1n}\\ \Delta\bar{q}_2\sigma_{21} & \omega_2 & \ddots & \Delta\bar{q}_2\sigma_{2n}\\ \vdots & \ddots & \ddots & \vdots\\ \Delta\bar{q}_n\sigma_{n1} & \Delta\bar{q}_n\sigma_{n2} & \cdots & \omega_n \end{pmatrix}. \quad (14)$$

Consider a nonsingular Hermitian matrix,

$$\mathbf{G}=\begin{pmatrix} \frac{1}{2k\Delta\bar{q}_1} & & \\ & \ddots & \\ & & \frac{1}{2k\Delta\bar{q}_n}\end{pmatrix}, \quad (15)$$

then the matrix

$$\mathbf{S}=\mathbf{GH}=\frac{1}{2k}\begin{pmatrix} \frac{\omega_1}{\Delta\bar{q}_1} & \sigma_{12} & \cdots & \sigma_{1n}\\ \sigma_{21} & \frac{\omega_2}{\Delta\bar{q}_2} & \ddots & \sigma_{2n}\\ \vdots & \ddots & \ddots & \vdots\\ \sigma_{n1} & \sigma_{n2} & \cdots & \frac{\omega_n}{\Delta\bar{q}_n}\end{pmatrix} \quad (16)$$

is also Hermitian since $\sigma_{ij}=\sigma_{ji}$. The Hamiltonian in Eq. (10) can be rewritten as

$$H(\boldsymbol{q})=\boldsymbol{q}^\dagger\mathbf{S}\boldsymbol{q}, \quad (17)$$

where $\boldsymbol{q}^\dagger$ is the conjugate transpose of $\boldsymbol{q}$. The complex canonical Hamiltonian equation has the form

$$\dot{\boldsymbol{q}}=-i\mathbf{G}^{-1}\frac{\partial H}{\partial \boldsymbol{q}^*}. \quad (18)$$

The system conserves two constants of motion: one is the Hamiltonian $H(\boldsymbol{q})$ and the other is the total wave action $I(\boldsymbol{q})$. Define an indefinite inner product [18,19] as

$$[\boldsymbol{x},\boldsymbol{y}]=(\mathbf{G}\boldsymbol{x},\boldsymbol{y})=\boldsymbol{y}^\dagger\mathbf{G}\boldsymbol{x}, \quad (19)$$

then the total wave action can be written as

$$I(\boldsymbol{q})=\sum_{i=1}^{n}\frac{Q_i^2}{2k\Delta\bar{q}_i}=\boldsymbol{q}^\dagger\mathbf{G}\boldsymbol{q}=[\boldsymbol{q},\boldsymbol{q}]. \quad (20)$$

For finite-dimensional systems, a matrix $\mathbf{H}$ is called pseudo-Hermitian [23,25] if $\mathbf{H}$ is similar to its conjugate transpose $\mathbf{H}^\dagger$ with

$$\mathbf{H}=\mathbf{G}^{-1}\mathbf{H}^\dagger\mathbf{G}, \quad (21)$$

where $\mathbf{G}$ is a nonsingular Hermitian matrix. Also, the matrix $\mathbf{A}=-i\mathbf{H}$ is called G-Hamiltonian [18–21,23] if there exists a nonsingular Hermitian matrix $\mathbf{G}$ and a Hermitian matrix $\mathbf{S}$, such that $\mathbf{A}=-i\mathbf{G}^{-1}\mathbf{S}$. Note that these two concepts are equivalent by definition [23], so that it is convenient to apply the stability theory of G-Hamiltonian matrices to pseudo-Hermitian systems [21,22].

We have thus shown that the dynamical system of n coupled vorticity waves given by Eq. (12) is a pseudo-Hermitian system. The diagonal terms of the system are isolated vorticity waves $\omega_i=kU_i+\Delta\bar{q}_i/2$, whereas the off-diagonal components $\Delta\bar{q}_i\sigma_{ij}$ and $\Delta\bar{q}_j\sigma_{ji}$ are nonreciprocal, non-Hermitian spatial coupling terms. Therefore, isolated vorticity waves form the Hermitian component of the system and correspond one to one to the eigenmodes of $\mathbf{H}$.

III. KREIN SIGNATURES AND KREIN COLLISION

In this section, we demonstrate how the mechanism of vorticity wave interaction is related to the stability theory of pseudo-Hermitian systems. We illustrate the Krein signatures of eigenvalues as the signs of the action of the corresponding vorticity waves. Therefore, the stability of eigenmodes is interpreted in terms of wave interaction [3,10], and the Krein collision between eigenvalues is interpreted as the interaction of positive-action and negative-action vorticity waves.

A. Stability of pseudo-Hermitian systems

Consider the eigensystem of a pseudo-Hermitian matrix, $\mathbf{H}\boldsymbol{u}=E\boldsymbol{u}$. The eigenvalues are symmetric with respect to the real axis, so that the eigenspectrum contains either purely real eigenvalues or complex-conjugate pairs. The eigenvalues of a pseudo-Hermitian matrix $\mathbf{H}$ are categorized as follows [18,21,22]:

(i) A real eigenvalue E is called definite with positive Krein signature $\kappa(E)=+1$, if $[\boldsymbol{u},\boldsymbol{u}]>0$ for any eigenvector $\boldsymbol{u}$ in its eigensubspace. It is called definite with negative Krein signature $\kappa(E)=-1$, if $[\boldsymbol{u},\boldsymbol{u}]<0$ for any eigenvector $\boldsymbol{u}$ in its eigensubspace.

(ii) A real eigenvalue E is called indefinite with Krein signature $\kappa(E)=0$, if there exists an eigenvector $\boldsymbol{u}$ in its eigensubspace, such that $[\boldsymbol{u},\boldsymbol{u}]=0$.

(iii) For a complex eigenvalue E with $\mathrm{Im}(E)\neq 0$, there is always $[\boldsymbol{u},\boldsymbol{u}]=0$. It is also assigned with a Krein signature $\kappa(E)=\pm 1$ when $\mathrm{Im}(E)\lessgtr 0$.

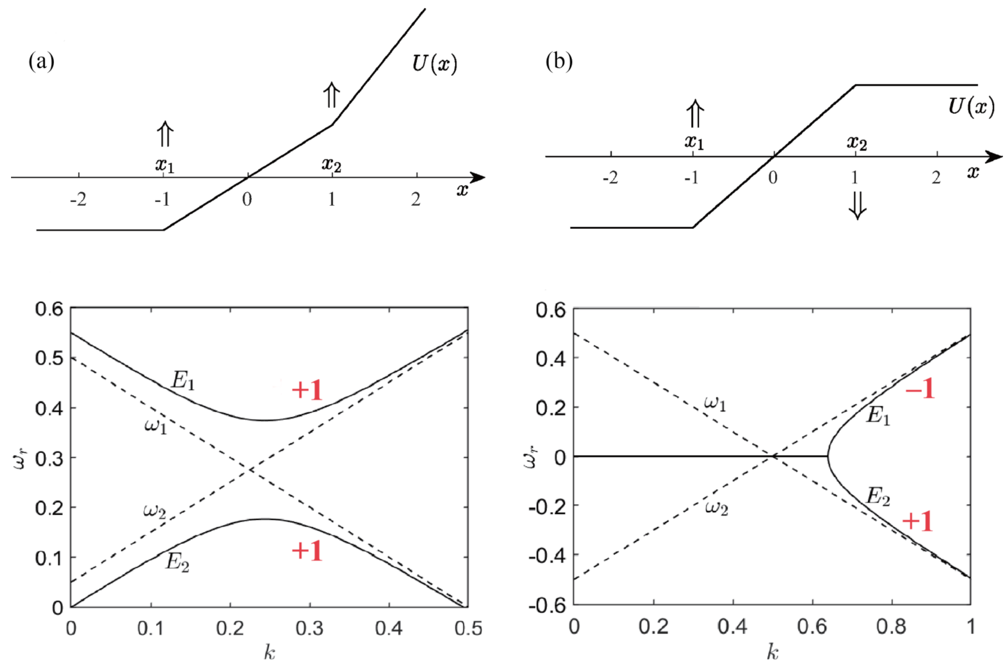

FIG. 1. Examples of two-interface shear layer profiles $U(x)$, with the dispersion relations of isolated vorticity waves $\omega_r(k)$ (dashed lines) and the real part of the corresponding eigenvalue branches $\mathrm{Re}(E) - k$ (solid lines). (a) A piecewise profile that supports two copropagating vorticity waves, with $\Delta\bar{q}_1 = 1$ and $\Delta\bar{q}_2 = 0.1$. (b) A piecewise profile that supports two counterpropagating vorticity waves, with $\Delta\bar{q}_1 = 1$ and $\Delta\bar{q}_2 = -1$. The eigenvalue branches are labeled with their Krein signatures.

We then recall the following properties of pseudo-Hermitian matrices [18]:

Theorem 1. For a pseudo-Hermitian matrix **H**, if the matrix **G** has p positive eigenvalues and q negative eigenvalues, then **H** has p eigenvalues with Krein signature $+1$ and q eigenvalues with Krein signature -1.

Theorem 2 (Krein-Gel'fand-Lidskii theorem). A pseudo-Hermitian system $\dot{\boldsymbol{q}} = -i\mathbf{H}\boldsymbol{q}$ is strongly stable (i.e., the stability of the system is preserved by any infinitesimal deformation of the Hamiltonian operator **H**) if and only if all eigenvalues of **H** are real and definite.

The proofs can be found in Ref. [18]. An immediate corollary is that for a pseudo-Hermitian system, while varying system parameters, the only route to become unstable is through the overlap between two definite eigenvalues with opposite Krein signatures on the real axis, known as the Krein collision [18–23]. The eigenvalues then move off the real axis and split into complex-conjugate pairs, leading to instabilities.

A physical interpretation of the Krein signature is the sign of the action of the corresponding eigenmode [21]. From Eqs. (17) and (19), we obtain

$$[\boldsymbol{u}, \boldsymbol{u}] = \frac{H(\boldsymbol{u})}{E}, \tag{22}$$

which is the ratio between the Hamiltonian and eigenfrequency of an eigenmode. Therefore, the Krein signature is illustrated as the sign of the action of the corresponding eigenmode, and the Krein collision is interpreted as the interaction between a positive-action mode and a negative-action mode [21].

In our system, the matrix **G** is closely related to the conserved total wave action $I(\boldsymbol{q}) = \boldsymbol{q}^\dagger \mathbf{G}\boldsymbol{q}$. Theorem 1 states that the Krein signatures of the eigenvalues of **H** are decided by the signs of $\Delta\bar{q}_i$, with

$$\sum_{i=1}^{n} \kappa(E_i) = \sum_{i=1}^{n} \mathrm{sign}(\Delta\bar{q}_i) = p - q. \tag{23}$$

Therefore, the Krein signatures of the eigenvalues are further illustrated as the signs of the action of the corresponding vorticity waves. If the system contains n copropagating vorticity waves with positive (negative) actions, then **G** is positive (negative) definite, all eigenvalues of **H** have the same Krein signature, and the system is stable. A necessary condition for instability of the system is that the background flow profile induces counterpropagating vorticity waves with opposite signs of actions, i.e., $|p - q| < n$. In other words, stability of the pseudo-Hermitian system is determined by its Hermitian component, characterized by the signs of $\Delta\bar{q}_i$. We have thus related the stability of eigenmodes to the properties of isolated vorticity waves.

B. Krein signatures of eigenvalue branches

1. The two-level system

In general, a two-level system is the building block of the dynamical system of n vorticity waves. Therefore, we first consider a flow profile with two interfaces, as shown in Fig. 1, to illustrate our main results. The flow profile is nondimensionalized with the characteristic scale length $L_* = \Delta x/2$ and characteristic velocity $V_* = \Delta U/2$, where $\Delta x = x_2 - x_1$ and $\Delta U = U(x_2) - U(x_1)$. The two-level vorticity wave system is

$$\dot{\boldsymbol{q}} = -i\mathbf{H}\boldsymbol{q}, \quad \boldsymbol{q} = \begin{pmatrix} q_1 \\ q_2 \end{pmatrix}, \tag{24}$$

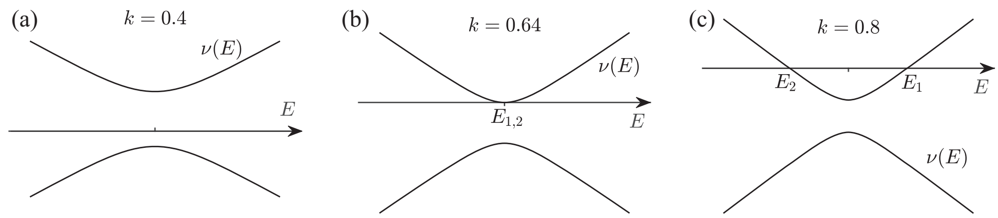

FIG. 2. Graphical interpretation of the Krein signatures in Fig. 1(b), with two eigenvalue branches of the pencil $\mathcal{L}$ at (a) $k = 0.4$, (b) $k = k_c \simeq 0.64$, and (c) $k = 0.8$. The zeros of the eigenvalue branches correspond to purely real eigenvalues of $\mathbf{H}$.

the Hamiltonian operator is

$$\mathbf{H} = \begin{pmatrix} \omega_1 & \Delta\bar{q}_1\sigma \\ \Delta\bar{q}_2\sigma & \omega_2 \end{pmatrix} \tag{25}$$

with $\sigma_{12} = \sigma_{21} \equiv \sigma$, and the eigenvalue relation is

$$(E - \omega_1)(E - \omega_2) = \Delta\bar{q}_1\Delta\bar{q}_2\sigma^2 \equiv \varepsilon. \tag{26}$$

When $\varepsilon \to 0$, the solutions are just isolated vorticity waves, $\omega_{1,2}(k)$. When $\varepsilon \neq 0$, the solutions are eigenvalue branches,

$$E_{1,2} = \frac{\omega_1 + \omega_2}{2} \pm \frac{1}{2}\sqrt{(\omega_1 - \omega_2)^2 + 4\varepsilon}. \tag{27}$$

The stability of the eigenmodes is decided by

$$\mathbf{G} = \begin{pmatrix} \frac{1}{2k\Delta\bar{q}_1} & 0 \\ 0 & \frac{1}{2k\Delta\bar{q}_2} \end{pmatrix}. \tag{28}$$

When $\Delta\bar{q}_1$ and $\Delta\bar{q}_2$ have the same sign, $\varepsilon > 0$ and the profile supports two copropagating vorticity waves, as shown in Fig. 1(a). The operator $\mathbf{H}$ remains quasi-Hermitian [25] and the eigenvalues $E_{1,2}$ are real with the same Krein signatures, so that there is no Krein collision. The two eigenvalue branches $E_{1,2}(k)$ approach each other near the intersection point without crossing, only with their corresponding vorticity waves exchanged from $\omega_1(\omega_2)$ to $\omega_2(\omega_1)$ [3]. When $\Delta\bar{q}_1$ and $\Delta\bar{q}_2$ have opposite signs, $\varepsilon < 0$ and the profile supports two counterpropagating vorticity waves, as shown in Fig. 1(b). The operator $\mathbf{H}$ is non-Hermitian and the eigenvalues have opposite Krein signatures. The Krein collision then corresponds to the interaction between positive-action and negative-action vorticity waves. The two eigenvalues become complex conjugates when $(\omega_1 - \omega_2)^2 + 4\varepsilon < 0$, i.e., $k < k_c \simeq 0.64$, characteristic of Kelvin-Helmholtz instabilities.

Therefore, the well-known Rayleigh's condition [36] for instability is equivalent to the condition of opposite Krein signatures, which requires the flow profile to have an inflection point. In terms of wave interaction, the flow profile is required to support counterpropagating vorticity waves [10]. Note that this condition is not sufficient for Kelvin-Helmholtz instabilities. The Fjørtoft's condition [36] requires that $U''(U - U_s) < 0$ somewhere within the flow domain, where $U_s = U(x_s)$ and x_s is the inflection point. In terms of wave interaction, this condition requires that the dispersion relations $\omega_1(k)$ and $\omega_2(k)$ intersect when $k > 0$. The details are referred to Ref. [10].

The Krein collision can also be illustrated from a graphical interpretation of the Krein signatures [40]. Consider a Hermitian linear pencil $\mathcal{L} = \mathbf{S} - E\mathbf{G}$, and solve the eigenvalue problem

$$\mathcal{L}(E)\boldsymbol{u}(E) = (\mathbf{S} - E\mathbf{G})\boldsymbol{u}(E) = \nu(E)\boldsymbol{u}(E), \tag{29}$$

parameterized by $E \in \mathbb{R}$, where $\nu = \nu(E)$ is called an eigenvalue branch of $\mathcal{L}$. The intersection points of $\nu(E)$ with the $\nu = 0$ axis then correspond to real eigenvalues of $\mathbf{H}$. Differentiate Eq. (29) at $E = E_i$ with $\nu(E_i) = 0$; we then obtain

$$(\mathbf{S} - E_i\mathbf{G})\boldsymbol{u}'(E_i) = \nu'(E_i)\boldsymbol{u}(E_i) + \mathbf{G}\boldsymbol{u}(E_i). \tag{30}$$

Taking the inner product with $\boldsymbol{u}(E_i)$ then gives

$$\nu'(E_i)(\boldsymbol{u}, \boldsymbol{u}) = -(\mathbf{G}\boldsymbol{u}, \boldsymbol{u}), \tag{31}$$

so that

$$\kappa(E_i) = -\text{sign}[\nu'(E_i)]. \tag{32}$$

Therefore, we can determine the Krein signatures of the real eigenvalues of $\mathbf{H}$ simply by the sign of the slope of $\nu(E)$ at the intersection points. For the system shown in Fig. 1(b), we plot $\nu(E)$ for specific choices of the parameter k in Fig. 2. When $k > k_c$, there are two intersection points with opposite signs of the slope, corresponding to two real eigenvalues of $\mathbf{H}$ that are definite with opposite Krein signatures, and the system is stable. When $k \to k_c$, the pair of intersection points overlap, which is the Krein collision. When $k < k_c$, the branches $\nu(E)$ have no zeros and the system is unstable.

2. The three-level system

In general, the stability of the $n \times n$ pseudo-Hermitian system given by Eq. (12) is determined by the signs of actions of the n vorticity waves. The coupling strength σ_{ij} decays exponentially with the distance between interfaces, so that the dominant off-diagonal terms are the coupling between neighboring vorticity waves. Therefore, Krein collisions between any of the adjacent eigenvalues can be approximately illustrated as the interaction between neighboring vorticity waves.

As a concrete example, consider the stability of three-interface piecewise profiles, as shown in Fig. 3. The profiles are nondimensionalized similarly to Fig. 1. The Hamiltonian operator of the dynamical system is

$$\mathbf{H} = \begin{pmatrix} \omega_1 & \Delta\bar{q}_1\sigma_1 & \Delta\bar{q}_1\sigma_2 \\ \Delta\bar{q}_2\sigma_1 & \omega_2 & \Delta\bar{q}_2\sigma_1 \\ \Delta\bar{q}_3\sigma_2 & \Delta\bar{q}_3\sigma_1 & \omega_3 \end{pmatrix}, \tag{33}$$

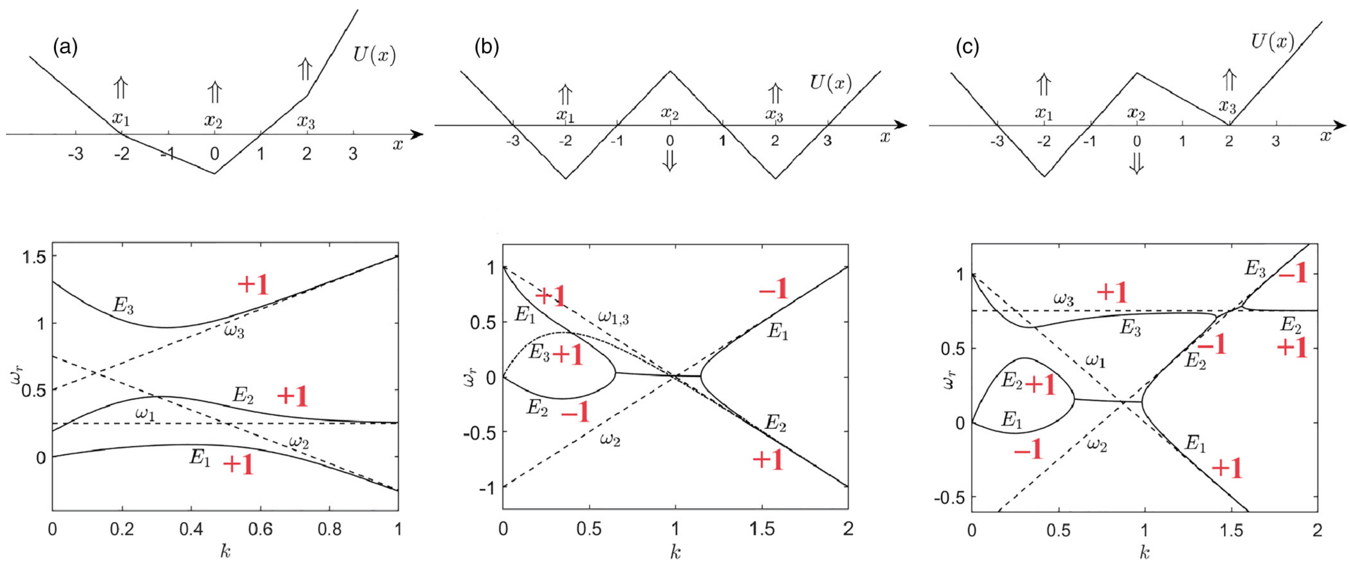

FIG. 3. Examples of three-interface piecewise profiles $U(x)$, the dispersion relations of isolated vorticity waves, $\omega_r(k)$ (dashed lines), and the real part of the corresponding eigenvalue branches, $\mathrm{Re}(E) - k$ (solid lines). (a) A piecewise profile that supports three copropagating vorticity waves, with $\Delta\bar{q}_1 = 1/2$, $\Delta\bar{q}_2 = 3/2$, and $\Delta\bar{q}_3 = 1/2$. (b) A symmetric jet profile that supports three counterpropagating vorticity waves, with $\Delta\bar{q}_1 = 2$, $\Delta\bar{q}_2 = -2$, and $\Delta\bar{q}_3 = 2$. (c) An asymmetric jet profile with $\Delta\bar{q}_1 = 2$, $\Delta\bar{q}_2 = -3/2$, and $\Delta\bar{q}_3 = 3/2$. The eigenvalue branches are labeled with their Krein signatures.

with $\sigma_{12} = \sigma_{23} \equiv \sigma_1 = e^{-2k}/2$ and $\sigma_{13} \equiv \sigma_2 = e^{-4k}/2$.

When $\Delta\bar{q}_{1,2,3}$ have the same sign, the profile supports three copropagating vorticity waves, as shown in Fig. 3(a). The eigenvalues $E_{1,2,3}$ are all definite with the same Krein signature, so that there is no Krein collision, and the eigenvalue branches approach each other without crossing. When $\Delta\bar{q}_2$ have opposite signs with $\Delta\bar{q}_{1,3}$, the profile supports counterpropagating vorticity waves. For the symmetric jet profile shown in Fig. 3(b), two Krein collisions are observed between the pair of eigenvalues of $E_{1,2}$ with opposite Krein signatures. Note that the vorticity waves ω_1 and ω_3 stand on an equal footing, so that the interaction between ω_2, ω_1 coincide with the interaction between ω_2, ω_3. Therefore, one of the eigenvalues E_3 remains neutrally stable, which corresponds to the varicose mode [10,36]. For the asymmetric jet profile shown in Fig. 3(c), there are two unstable ranges of parameters, corresponding to four Krein collisions. The eigenvalue branches $\nu(E)$ of the Hermitian pencil $\mathcal{L}$ are plotted in Fig. 4 and the Krein signatures in Fig. 3(c) are labeled accordingly.

Figures 1 and 3 illustrate the fact that the eigenmodes of $\mathbf{H}$ correspond one to one to the isolated vorticity waves, and the eigenvalue branches are infinitely close to isolated vorticity waves in the weak-coupling limit. In this limit, $\sigma_{ij} \to 0$ and the off-diagonal, non-Hermitian terms of $\mathbf{H}$ can be ignored. Then we have

$$\nu_i(E) = \frac{\omega_i - E}{2k\Delta\bar{q}_i}, \tag{34}$$

and the Krein signatures

$$\kappa_i(E) = -\mathrm{sign}[\nu_i'(E)] = \mathrm{sign}(\Delta\bar{q}_i) \tag{35}$$

are just the signs of the action of corresponding vorticity waves, as guaranteed by Theorem 1. We also conclude that when the control parameter k is varied across the intersection point of $\omega_i(k)$ and $\omega_j(k)$, the eigenvalue branches $E_{i,j}(k)$ will exchange their corresponding vorticity waves [3], so that the Krein signatures of $E_{i,j}(k)$ will also exchange.

IV. $\mathcal{PT}$-SYMMETRY BREAKING AND EXCEPTIONAL POINTS

Krein collision of eigenvalues is intimately related to symmetry-breaking bifurcations and the formation of EPs in pseudo-Hermitian systems [21–23,41]. In this section, we demonstrate that the model of vorticity wave interaction provides a clear physical description of $\mathcal{PT}$-symmetry breaking

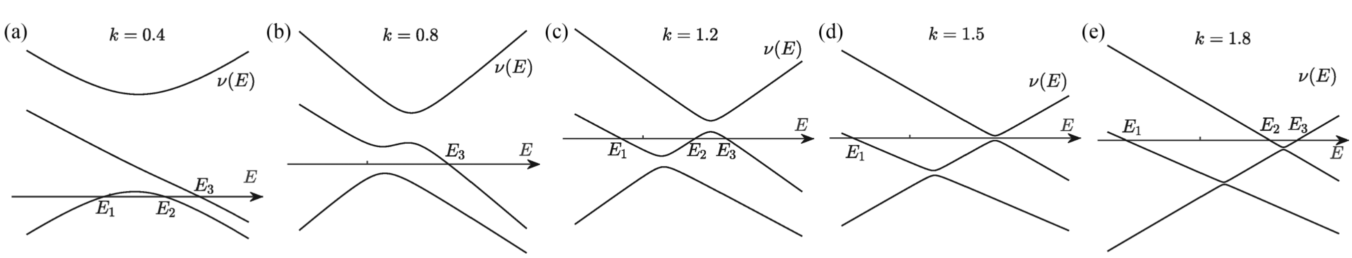

FIG. 4. Graphical interpretation of the Krein signatures in Fig. 3(c), with three eigenvalue branches of the pencil $\mathcal{L}$ at (a) $k = 0.4$, (b) $k = 0.8$, (c) $k = 1.2$, (d) $k = 1.5$, and (e) $k = 1.8$. The zeros of the eigenvalue branches correspond to purely real eigenvalues of $\mathbf{E}$.

and the formation of EPs in Kelvin-Helmholtz instabilities. We also describe the critical behavior around the EPs from the phase dynamics of vorticity waves.

A. Krein collision, $\mathcal{PT}$-symmetry breaking, and formation of exceptional points

We first show that the dynamical system of coupled vorticity waves is $\mathcal{PT}$ symmetric. For the system of n vorticity waves, the parity operator $\mathcal{P}$ and the time-reversal operator $\mathcal{T}$ acting on vorticity perturbations $\boldsymbol{q}$ are

$$\mathcal{P} = \begin{pmatrix} -1 & & \\ & \ddots & \\ & & -1 \end{pmatrix} \quad \text{and} \quad \mathcal{T} = \mathcal{K}, \tag{36}$$

satisfying $\mathcal{P}^2 = \mathcal{T}^2 = \mathcal{I}_{n\times n}$, where $\mathcal{K}$ is the complex-conjugate operator and $\mathcal{I}$ the identity operator. The parity operator $\mathcal{P}$ defined here performs a reflection about the x axis. One can readily see that the Hamiltonian operator $\mathbf{H}$ is $\mathcal{PT}$ symmetric, i.e., $\mathcal{PT}\mathbf{H} - \mathbf{H}\mathcal{PT} = 0$. The following theorem relates the concepts of pseudo-Hermiticity and $\mathcal{PT}$ symmetry:

Theorem 3. For a finite-dimensional system, a $\mathcal{PT}$-symmetric Hamiltonian operator $\mathbf{H}$ is necessarily pseudo-Hermitian.

The proof can be found in Ref. [23]. It follows that $\mathcal{PT}$-symmetric operators constitute a subclass of pseudo-Hermitian operators [25].

In general, a linear operator system can yield solutions with less symmetry than its governing equations [13,14]. Consider the eigensystem of a $\mathcal{PT}$-symmetric operator $\mathbf{H}\boldsymbol{u}_i = E_i\boldsymbol{u}_i$. When all eigenvalues E_i are real, we obtain

$$\mathbf{H}\mathcal{PT}\boldsymbol{u}_i = E_i^*\mathcal{PT}\boldsymbol{u}_i = E_i\mathcal{PT}\boldsymbol{u}_i, \tag{37}$$

so that $\boldsymbol{u}_i$ is also an eigenvector of the joint operator $\mathcal{PT}$, and the $\mathcal{PT}$ symmetry is unbroken. When E_i becomes complex, then $\boldsymbol{u}_i$ is no longer an eigenvector of $\mathcal{PT}$, and the $\mathcal{PT}$ symmetry is broken. The boundaries that separate the parameter space of broken and unbroken $\mathcal{PT}$ symmetry are called EPs, where the real eigenvalues are degenerate and the corresponding eigenvectors coalesce [26].

In terms of pseudo-Hermiticity, the only route to the spontaneous breaking of $\mathcal{PT}$ symmetry and formation of EPs is through the Krein collision between eigenvalues [22]. Denote the eigenvectors of $\mathbf{H}^\dagger$ as $\mathbf{H}^\dagger\boldsymbol{v}_i = E_i^*\boldsymbol{v}_i$, then the biorthogonal relation [25] gives

$$\boldsymbol{v}_i^\dagger\boldsymbol{u}_j = \delta_{ij}. \tag{38}$$

When all eigenvalues E_i are real and nondegenerate, combined with $\mathbf{H}^\dagger\mathbf{G}\boldsymbol{u}_i = E_i\mathbf{G}\boldsymbol{u}_i$, we have $\mathbf{G}\boldsymbol{u}_i = c\boldsymbol{v}_i$ and

$$[\boldsymbol{u}_i, \boldsymbol{u}_i] = \boldsymbol{u}_i^\dagger\mathbf{G}\boldsymbol{u}_i = c\boldsymbol{v}_i^\dagger\boldsymbol{u}_i = c, \tag{39}$$

where c is a nonzero real constant. Therefore, all eigenvalues of $\mathbf{H}$ are definite and belong to class (i), with Krein signatures $\kappa(E_i) = \pm 1$.

When the control parameter is varied so that the eigenvalue E_i is degenerate, there are two possibilities. If the degeneracy is between two eigenvalues with the same Krein signature, it forms a diabolic point (DP), where the eigenvectors remain complete and orthogonal [25]. The eigenvalue E_i then remains real and definite. If the degeneracy is between two eigenvalues with opposite Krein signatures, it forms an EP where the eigenvectors also coalesce and become identical. At an EP, the geometric multiplicity of E_i is less than its algebraic multiplicity, and there exists an eigenvector such that $[\boldsymbol{u}_i, \boldsymbol{u}_i] = 0$ [19,22], so that E_i is indefinite and belongs to class (ii), with Krein signature $\kappa(E_i) = 0$.

Krein collision between two eigenvalues with opposite Krein signatures then corresponds to the formation of EPs, the emergence of complex eigenvalues, and the breaking of $\mathcal{PT}$ symmetry. When E_i becomes complex, we denote $E_j = E_i^*$ and obtain $\mathbf{G}\boldsymbol{u}_j = c\boldsymbol{v}_i$, so that

$$[\boldsymbol{u}_j, \boldsymbol{u}_j] = \boldsymbol{u}_j^\dagger\mathbf{G}\boldsymbol{u}_j = c\boldsymbol{v}_i^\dagger\boldsymbol{u}_j = 0. \tag{40}$$

Therefore, the complex eigenvalue E_i belong to class (iii).

We thus conclude that in $\mathcal{PT}$-symmetric systems, the mechanism of $\mathcal{PT}$-symmetry breaking and the formation of EPs is through Krein collision between definite eigenvalues with opposite Krein signatures [22,23]. When the control parameter is varied across the EP, the system undergoes a $\mathcal{PT}$-symmetry-breaking bifurcation [24].

B. Dynamical system of two counterpropagating vorticity waves

We now illustrate these results within the dynamical system of two counterpropagating vorticity waves. For the flow profile shown in Fig. 1(b), the dispersion relations of isolated vorticity waves are $\omega_1 = -k + 1/2$, $\omega_2 = k - 1/2$, and the coupling coefficient is $\sigma = e^{-2k}/2$. Denote the frequency mismatch $\Delta\omega = \omega_1 - \omega_2 = 1 - 2k$, then the eigenvalues of $\mathbf{H}$ are

$$E_{1,2} = \pm\tfrac{1}{2}\sqrt{\Delta\omega^2 - 4\sigma^2}, \tag{41}$$

and the eigenvectors

$$\boldsymbol{u}_{1,2} = \begin{pmatrix} -\frac{\Delta\omega}{2\sigma} \mp \frac{\sqrt{\Delta\omega^2 - 4\sigma^2}}{2\sigma} \\ 1 \end{pmatrix}. \tag{42}$$

Denote the discriminant of the characteristic polynomial of $\mathbf{H}$ as

$$D = \Delta\omega^2 - 4\sigma^2 = (2k-1)^2 - e^{-4k}. \tag{43}$$

For $k > k_c$, $D > 0$ and the eigenvalues $E_{1,2}$ are real and definite with opposite Krein signatures. The eigenvectors $\boldsymbol{u}_{1,2}$ are also eigenvectors of $\mathcal{PT}$, with $\mathcal{PT}\boldsymbol{u} = -\boldsymbol{u}^* = -\boldsymbol{u}$, so that the system has unbroken $\mathcal{PT}$ symmetry. For $0 < k < k_c$, $D < 0$ and $\mathbf{H}$ has a pair of complex-conjugate eigenvalues $E_{1,2} = -i\sigma\sin\theta_{12}$. The eigenvectors $\boldsymbol{u}_{1,2} = (e^{i\theta_{12}} \;\; 1)^T$ are no longer eigenvectors of $\mathcal{PT}$, so that $\mathcal{PT}$ symmetry is broken.

The boundary of this change is marked by the EP at $k = k_c$, where $D = 0$ and $E_{1,2}$, $\boldsymbol{u}_{1,2}$ are identical. As shown in Fig. 5, the EP is a saddle point in the complex $E - k$ space, and the onset of Kelvin-Helmholtz instability is via bifurcation through the EP.

The control parameter of this $\mathcal{PT}$-symmetry-breaking bifurcation can be illustrated from spatial coupling of vorticity

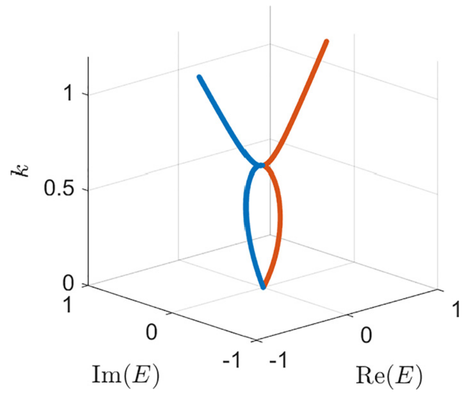

FIG. 5. The eigenvalues $E_1(k)$ (red) and $E_2(k)$ (blue) in the complex [Re(E), Im(E), k] space. The saddle-node exceptional point locates at $k = k_c$.

waves. Consider the amplitude-phase form [8,11] of the dynamical system,

$$\dot{Q}_1 = -\sigma Q_2 \sin\theta_{12}, \quad \dot{Q}_2 = -\sigma Q_1 \sin\theta_{12}, \tag{44a}$$

$$\dot{\theta}_1 = -\omega_1 - \sigma\frac{Q_2}{Q_1}\cos\theta_{12}, \quad \dot{\theta}_2 = -\omega_2 + \sigma\frac{Q_1}{Q_2}\cos\theta_{12}. \tag{44b}$$

Let $R_{12} = Q_1/Q_2$, and rewrite the dynamical system as

$$\dot{R}_{12} = \sigma\left(R_{12}^2 - 1\right)\sin\theta_{12}, \tag{45a}$$

$$\dot{\theta}_{12} = -\Delta\omega - \sigma\left(R_{12} + \frac{1}{R_{12}}\right)\cos\theta_{12}. \tag{45b}$$

The fixed points of the system require either

$$\sin\theta_{12} = 0, \quad R_{12} + \frac{1}{R_{12}} = \frac{\Delta\omega}{\sigma\cos\theta_{12}}, \tag{46}$$

where the two vorticity waves remain neutrally stable, or

$$R_{12} = 1, \quad \cos\theta_{12} = -\frac{\Delta\omega}{2\sigma}, \tag{47}$$

where the two vorticity waves are phase locked. The control parameter of the bifurcation of fixed points is then the ratio between frequency detuning and coupling strength of the vorticity waves,

$$\mu = -\frac{\Delta\omega}{2\sigma} = (2k-1)e^{2k}. \tag{48}$$

Note that μ is a monotonously increasing function of k when $k \geqslant 0$, so that the parameter space for $\mathcal{PT}$-symmetry breaking and instability onset $-1 < \mu < 1$ is equivalent to $0 < k < k_c \simeq 0.64$, as shown in Fig. 6.

Therefore, the onset of Kelvin-Helmholtz instability corresponds to the bifurcation of fixed points from two neutral centers to a pair of stable and unstable nodes [11]. Note that the fixed points are equivalent to the normal mode solutions $\boldsymbol{u}_1 e^{-iE_1 t}$ and $\boldsymbol{u}_2 e^{-iE_2 t}$. When $k > k_c$, the system has two neutrally stable fixed points, and neither eigenmode is dominant. When $0 < k < k_c$, the phase locking of two vorticity waves corresponds to a pair of stable and unstable fixed points, depending on the sign of $\sin\theta_{12}$. The $-\pi < \theta_{12} < 0$ fixed point corresponds to the unstable eigenmode, which leads to

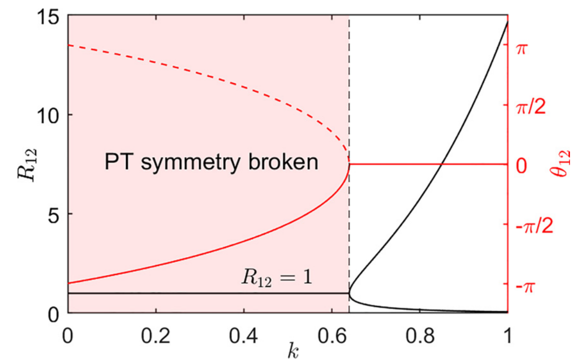

FIG. 6. Parameter space of the two vorticity wave system and bifurcation of fixed points with the control parameter k. The black vertical dashed line is the critical $k = k_c \simeq 0.64$. When $k \geqslant k_c$, the system has two neutrally stable fixed points, located at $\theta_{12} = 0$, with unbroken $\mathcal{PT}$ symmetry. When $0 < k < k_c$, the system has a pair of stable (solid red line, $-\pi < \theta_{12} < 0$) and unstable (dashed red line, $0 < \theta_{12} < \pi$) fixed points, and $\mathcal{PT}$ symmetry is spontaneously broken.

the mutual growth of vorticity waves, and naturally dominates in long-term dynamics. This fixed point is thus stable as a dynamical sink of phase plane trajectories. The $0 < \theta_{12} < \pi$ fixed point corresponds to the stable eigenmode, which leads to the mutual damping of initial perturbations. This fixed point is thus unstable as a source of phase plane trajectories [11].

In general, we have shown that the control parameter of the $\mathcal{PT}$-symmetry-breaking bifurcation is the ratio $\mu = -\frac{\Delta\omega}{2\sigma}$, which measures the competition between frequency detuning and coupling strength of vorticity waves. This parameter increases monotonously with k, which is the nondimensionalized wave number of perturbations. When the coupling strength dominates over phase detuning, the parameter space $0 < k < k_c$ corresponds to phase-locking and mutual growth of vorticity waves. When the coupling is weak compared to the phase detuning, the parameter space $k > k_c$ corresponds to neutrally stable vorticity waves. The physical meaning of k is the wavelength of vorticity waves compared to the distance between the vorticity jump interfaces [10]. When $k\Delta x \gg 1$, the distance between adjacent vorticity waves is too large compared to their wavelength, so that the waves do not feel each other's presence as if they were isolated.

It is interesting to compare the results above to the $\mathcal{PT}$-symmetry analysis in Ref. [16], where velocity perturbations are used as the field variable. It is shown in [16] that when the system is stable with unbroken $\mathcal{PT}$ symmetry, the phase difference between $\hat{v}_x(x,t)$ and $\hat{v}_y(x,t)$ is locked to $\pi/2$, and when the system is unstable with broken $\mathcal{PT}$ symmetry, the phase difference becomes arbitrary and spatially dependent. In our work, using vorticity perturbations as the field variable, we show that when the system is unstable, both eigenmodes are phase locked to $-\pi < \theta_{12} < 0$, and the normal mode solution

$$\hat{\phi}(x,t) = -\left(\frac{e^{i\theta_{12}}e^{-k|x+1|} + e^{-k|x-1|}}{2k}\right)e^{-\sigma\sin\theta_{12}t} \tag{49}$$

has a rather complicated mode structure. Therefore, $\hat{v}_x = -ik\hat{\phi}$ and $\hat{v}_y = \hat{\phi}'$ are phase locked in time, but with an arbitrary and spatially dependent phase difference. When the system is stable with unbroken $\mathcal{PT}$ symmetry, both eigenmodes are phase locked to $\theta_{12} = 0$, so that $\theta_1 = \theta_2 \equiv \theta(t)$ and $\hat{\phi}(x,t) = |\hat{\phi}(x)|e^{i[\theta(t)+\pi]}$. Therefore, $\hat{v}_x = -ik\hat{\phi}$ and $\hat{v}_y = \hat{\phi}'$ are phase locked to $\pi/2$, which is consistent with Ref. [16].

However, we emphasize that when the $\mathcal{PT}$ symmetry is unbroken, both eigenmodes are neutrally stable and neither is dominant, so that the physical solution $\boldsymbol{q}(t)$ does not converge to any of the normal modes. The nonorthogonality of eigenvectors near the EP then leads to transient phase-slip dynamics, which is an intriguing feature of the EP and beyond the scope of [16].

C. Critical behavior around the exceptional point

One of the most striking features of non-Hermitian systems is the existence of EPs. In Hermitian systems, the critical point where the eigenvalues degenerate is a DP, where the eigenvalues are identical but the eigenvectors remain complete and orthogonal. At an EP, the eigenvectors also coalesce and become identical. This nonorthogonality of eigenvectors near the EP is a unique feature of non-Hermitian systems. The transient dynamics around the EP is actively investigated in the context of non-Hermitian optics and photonics, where power oscillations or amplifications have been observed [27]. These observations are closely related to the transient growth in fluid dynamics [35] and reveal a generic property that when a system operates around an EP, it becomes highly sensitive to perturbations of the system [24–26]. In this section, we demonstrate this characteristic of EP from the perspective of vorticity wave interaction and describe this transient behavior as a transition between phase-locking and phase-slip dynamics.

Denote the left and right eigenvectors of $\mathbf{H}$ as $\langle u^L|$ and $|u^R\rangle$, where $|u^R\rangle = \boldsymbol{u}$ and $\langle u^L| = \boldsymbol{v}^\dagger$. The eigenvectors of the non-Hermitian system are biorthonormal [25], with $\langle u_i^L|u_j^R\rangle = \delta_{ij}$. A quantitative measure for the nonorthogonality of the eigenvectors is the phase rigidity [26,42,43], defined as

$$r = \frac{\langle u^L|u^R\rangle}{\langle u^R|u^R\rangle}. \tag{50}$$

In Hermitian systems, the right eigenvectors are orthogonal and the phase rigidity $r = 1$. In non-Hermitian systems, the right eigenvectors of different states are skewed instead of orthogonal, and the phase rigidity is parameter dependent, with $|r| < 1$. Approaching the EP, the two eigenvectors coalesce and $r \to 0$. For the system of two counterpropagating vorticity waves,

$$\langle u_{1,2}^L| = \left(\frac{\Delta\omega}{2\sigma} \pm \frac{\sqrt{\Delta\omega^2 - 4\sigma^2}}{2\sigma} \quad 1 \right),$$

and the phase rigidity

$$|r_{1,2}| = \begin{cases} \sqrt{1 - \frac{4\sigma^2}{\Delta\omega^2}}, & k > k_c \\ \sqrt{1 - \frac{\Delta\omega^2}{4\sigma^2}}, & 0 < k < k_c \end{cases} \tag{51}$$

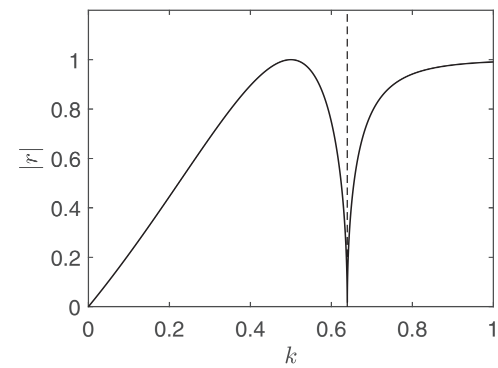

FIG. 7. Plot of the phase rigidity $|r|$ as a function of k. At the EP, $r = 0$ and the eigenvectors are identical. In the vicinity of the EP, $|r| \propto |k - k_c|^{1/2}$ and the eigenvectors are extremely nonorthogonal. When $k \gg k_c$, the coupling is weak and $|r| \to 1$. Note that at $k = 0.5$, the frequency mismatch of two vorticity waves vanishes and $|r| \simeq 1$.

is plotted in Fig. 7. Expand the phase rigidity near the EP and we obtain $|r_{1,2}| \propto |k - k_c|^{1/2}$. In the vicinity of the EP, the phase rigidity quantifies the splitting of eigenvectors [26], which follows a square-root dependence similar to the splitting of eigenvalues, $\delta E = |E_1 - E_2| \propto |k - k_c|^{1/2}$.

The critical exponent $s = 1/2$ is associated with the critical behavior of the vorticity wave dynamics near the EP. For an arbitrary initial condition, the amplitude and phase dynamics of the two vorticity waves can be obtained from the superposition of normal modes,

$$\boldsymbol{q}(t) = c_1\boldsymbol{u}_1 e^{-iE_1 t} + c_2\boldsymbol{u}_2 e^{-iE_2 t}, \tag{52}$$

as shown in Fig. 8. The parameter space $0 < k < k_c$ corresponds to phase-locking dynamics and exponential growth of initial perturbations, and the parameter space $k > k_c$ corresponds to phase-slip dynamics and transient growth of initial perturbations. When $k \gg k_c$, the vorticity waves decouple and remain neutrally stable.

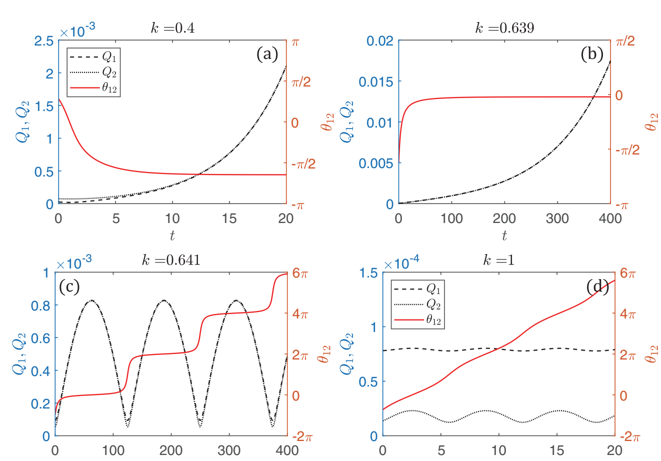

FIG. 8. The amplitude and phase dynamics of two coupled counterpropagating vorticity waves, calculated from Eqs. (44a) and (44b). The initial perturbations are random with amplitude $\sim 10^{-5}$. The control parameter of the system is (a) $k = 0.4$, (b) $k = 0.639 \sim k_c^-$, (c) $k = 0.641 \sim k_c^+$, and (d) $k = 1$.

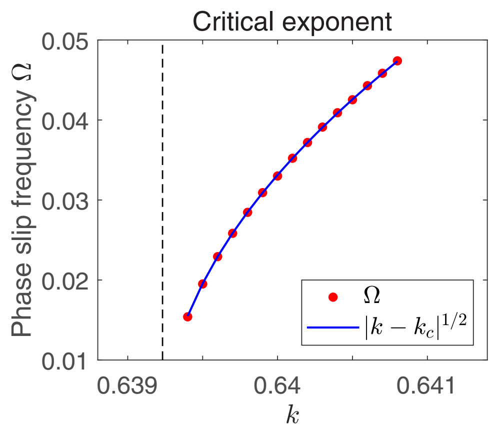

FIG. 9. The critical exponent of phase-slip frequency Ω near the EP is $s = 1/2$. The red dots are numerically calculated from Eqs. (44a) and (44b), and the solid blue line is $\propto |k - k_c|^{1/2}$.

Note that when the system crosses through the EP from $k = k_c^+$ to $k = k_c^-$, a transition of phase dynamics occurs from a phase-slip state [Fig. 8(c)] to a phase-locking state [Fig. 8(b)]. The transition is captured by

$$\dot{\theta}_{12} = -\Delta\omega - 2\sigma \cos\theta_{12}, \tag{53}$$

which is obtained from Eq. (45b) in the vicinity of the EP, where $R_{12} \to 1$.

Equation (53) is the Adler equation [30,31], which contains both phase-locking and phase-slip solutions. The phase-slip dynamics of $\theta_{12}(t)$ are highly nonuniform in time in the vicinity of the EP, and correspond to transient growth of the initial perturbations [7–9] in the regime of unbroken $\mathcal{PT}$ symmetry. Denote the phase-slip period T as the time required for θ_{12} to jump by 2π. For most of the time in the period, the dynamical phase θ_{12} is getting through the bottleneck around multiples of 2π, predicted by the neutrally stable fixed point when $k > k_c$. More precisely, θ_{12} is around $2n\pi^-$ in the first half of the period, which corresponds to transient growth, and around $2n\pi^+$ in the second half of the period, which corresponds to transient decay. A phase-slip period then ends with a short interval of 2π phase jump, so that the initial perturbations endure periodic oscillations of nonmodal growth and decay. When $k \gg k_c$ [Fig. 8(d)], the phase-slip period $T \to 2\pi/\Delta\omega$ and $\theta_{1,2}(t) \propto t$, the normal modes become orthogonal, and transient growth vanishes.

The phase-slip period T near the EP is estimated as

$$T = \int_0^{2\pi} \frac{d\theta_{12}}{-\Delta\omega - 2\sigma\cos\theta_{12}} = \frac{2\pi}{\sqrt{\Delta\omega^2 - 4\sigma^2}}, \tag{54}$$

and the phase-slip frequency $\Omega = \sqrt{\Delta\omega^2 - 4\sigma^2}$. Therefore, the phase-slip frequency satisfies $\Omega \propto |k - k_c|^{1/2}$ near the EP, following a square-root scaling law, as shown in Fig. 9. The results are consistent with the square-root dependence of the phase rigidity, showing that when the eigenvectors are extremely nonorthogonal, the phase dynamics become extremely nonmodal and highly nonuniform in time accordingly. The transition of phase dynamics thus provides a useful description of the critical behavior around the EP.

The transient growth of perturbations near the EP,

$$\frac{Q(t)}{Q(0)} = \exp\left[-\sigma\int_0^t \sin\theta_{12}(t)dt\right], \tag{55}$$

can also be estimated for the first half-period as

$$\frac{Q(\frac{T}{2})}{Q(0)} = \exp\left[-\sigma\int_{\cos\theta_0}^1 \frac{d\cos\theta_{12}}{\Delta\omega + 2\sigma\cos\theta_{12}}\right] = \sqrt{\frac{\mu - \cos\theta_0}{\mu - 1}}, \tag{56}$$

where $\theta_0 = \theta_{12}(0)$. The optimal amplification factor G for transient growth is then obtained when $\cos\theta_0 = -1$, as

$$G = \sqrt{\frac{\mu + 1}{\mu - 1}}. \tag{57}$$

We have thus recovered the optimal transient growth rate given by Eq. (57) that is consistent with previous results [7,8]. See the Appendix A for details. We also note that the nonmodal, transient growth of perturbations is a generic property at the threshold of the transition to instabilities when the eigenvectors are nonorthogonal [33,34], not limited to the breaking of $\mathcal{PT}$ symmetry.

In general, for n-vorticity wave systems, the stability of the system is determined by the signs of actions of the n vorticity waves, and the dominant off-diagonal coupling terms are the coupling between neighboring vorticity waves. When the system parameter is arbitrarily close to a second-order EP, the difference between neighboring E_i and E_j is arbitrarily small, so that only the two neighboring vorticity waves ω_i and ω_j are important in close vicinity of the EP. Therefore, a $\mathcal{PT}$-symmetry-breaking bifurcation can be approximately illustrated as a Krein collision between two neighboring eigenvalues and the spatial coupling between two counterpropagating waves. For adjacent vorticity waves ω_i and ω_j with opposite signs of actions, the phase difference is approximately

$$\dot{\theta}_{ij} = -\Delta\omega_{ij} + \sigma_{ij}(\Delta\bar{q}_j R_{ij} - \Delta\bar{q}_i R_{ji})\cos\theta_{ij}, \tag{58}$$

where only the spatial couplings between ω_i and ω_j are kept. Equation (58) also forms an Adler equation near the EP, where $R_{ij} \to$ const. The transition between phase-locking and phase-slip dynamics can then be observed at the boundaries of the Krein collisions between eigenvalues E_i and E_j. We conclude that the transition between phase-locking and phase-slip dynamics and the transient growth of perturbations describe the essential characteristics of EPs in shear flow instabilities, and that the square-root dependence is a universal characteristic of EPs in vorticity wave systems.

V. SUMMARY AND DISCUSSION

In this work, we relate the model of vorticity wave interaction to the analysis of Krein collision and $\mathcal{PT}$-symmetry breaking in shear flow instabilities. We show that the dynamical system of coupled vorticity waves is a pseudo-Hermitian system, and the eigenmodes of the system correspond one to one to the isolated vorticity waves. The Krein signatures of the eigenvalue branches are decided by the signs of action of the vorticity waves. The spatial coupling of counterpropagating vorticity waves illustrates the Krein collision between eigenvalues, the spontaneous breaking of $\mathcal{PT}$ symmetry, and the formation of EPs. The control parameter of $\mathcal{PT}$-symmetry breaking is shown to be the ratio between frequency detuning and coupling strength of the vorticity waves.

Critical behavior near the EPs is described as a transition between phase-slip and phase-locking dynamics of the vorticity waves. We show that this transition of phase dynamics corresponds to the spontaneous $\mathcal{PT}$-symmetry breaking and onset of shear instabilities. In particular, the highly nonuniform-in-time phase-slip dynamics corresponds to the extreme nonorthogonality of eigenvectors near the EPs, measured by the phase rigidity. The phase-slip dynamics lead to nonmodal, transient growth of perturbations near the EP in the regime of unbroken $\mathcal{PT}$ symmetry. The phase-slip frequency shares the same critical exponent 1/2 with the phase rigidity of system eigenvectors, indicating the square-root dependence as a universal characteristic of EPs in shear flow instabilities.

In general, we have shown that the framework of vorticity wave interaction is naturally related to non-Hermitian physics and $\mathcal{PT}$-symmetry-breaking bifurcations. We note that the interaction between positive-action and negative-action waves is a generic mechanism to explain reactive instabilities in plasmas [3,21]. Therefore, we anticipate further applications of this framework not limited to instabilities in shear flows, but also in magnetized plasmas, such as drift wave instabilities [37,41] and magnetohydrodynamic instabilities [44–46]. It would be interesting there to label the eigenmodes driven from various free-energy sources with their Krein signatures, to discuss how the stability of joint modes are shaped by the mechanism of wave interaction, and to understand how the plasmas behave near marginal stability from analysis of the EPs.

Note added. Recently, the authors become aware of a relevant paper [47] that relates the Krein signatures to the formation of EPs in pseudo-Hermitian systems.

ACKNOWLEDGMENTS

We acknowledge useful discussions with J. Q. Li, J. Wang, Z. J. Mao, Y. Zhang, and H. T. Chen. This work was supported by the National Natural Science Foundation of China with Grants No. 12075013, No. 12275071, and No. U1967206.

APPENDIX: TRANSIENT GROWTH ANALYSIS

In this Appendix, we discuss alternative approaches to obtain the transient growth rate [7,8,28,29,32] in the regime of unbroken $\mathcal{PT}$ symmetry, in comparison with the results estimated from phase-slip dynamics.

Given initial condition $\boldsymbol{q}(0) = \boldsymbol{q}_0$, the general solution of the initial value problem is $\boldsymbol{q}(t) = e^{\mathbf{A}t}\boldsymbol{q}_0$, and the propagator matrix of the dynamical system, $e^{\mathbf{A}t} = e^{-i\mathbf{H}t}$, can be obtained from the superposition of normal modes,

$$\begin{aligned} \boldsymbol{q}(t) &= c_1\boldsymbol{u}_1 e^{-iE_1 t} + c_2\boldsymbol{u}_2 e^{-iE_2 t}, \\ \boldsymbol{q}(0) &= c_1\boldsymbol{u}_1 + c_2\boldsymbol{u}_2. \end{aligned} \tag{A1}$$

The coefficients c_1, c_2 are readily solved from Eq. (A1), and one gets

$$e^{\mathbf{A}t} = \begin{pmatrix} \cos E_1 t - i\frac{\Delta\omega}{2E_1}\sin E_1 t & -i\frac{\sigma}{E_1}\sin E_1 t \\ i\frac{\sigma}{E_1}\sin E_1 t & \cos E_1 t + i\frac{\Delta\omega}{2E_1}\sin E_1 t \end{pmatrix}, \tag{A2}$$

where $E_1 = \sqrt{(\Delta\omega/2)^2 - \sigma^2}$. The amplification factor of transient growth under certain initial conditions is then

$$\begin{aligned} G^2(t) &= \frac{(\boldsymbol{q}(t), \boldsymbol{q}(t))}{(\boldsymbol{q}_0, \boldsymbol{q}_0)} = \frac{(e^{\mathbf{A}^\dagger t} e^{\mathbf{A}t}\boldsymbol{q}_0, \boldsymbol{q}_0)}{(\boldsymbol{q}_0, \boldsymbol{q}_0)} \\ &= \frac{|q_1(t)|^2 + |q_2(t)|^2}{|q_1(0)|^2 + |q_2(0)|^2}. \end{aligned} \tag{A3}$$

The optimal growth can be obtained either using the singular value decomposition (SVD) approach [7,32] or directly calculating $G^2(t)$ [28]. The SVD of $e^{\mathbf{A}t}$ has the form of $e^{\mathbf{A}t} = \mathbf{U}\mathbf{\Sigma}\mathbf{V}^\dagger$, where the columns of $\mathbf{U}$ and $\mathbf{V}$ are eigenvectors of $e^{\mathbf{A}t}e^{\mathbf{A}^\dagger t}$ and $e^{\mathbf{A}^\dagger t}e^{\mathbf{A}t}$, separately. In the regime of unbroken $\mathcal{PT}$ symmetry, the singular value matrix is

$$\Sigma = \begin{pmatrix} g & 0 \\ 0 & g^{-1} \end{pmatrix}, \quad g = \sqrt{\frac{\mu - \cos\theta_0}{\mu + \cos\theta_0}}, \tag{A4}$$

so that the optimal growth factor is

$$G = \sqrt{\frac{\mu + 1}{\mu - 1}}, \tag{A5}$$

with the optimal initial condition $Q_1(0) = Q_2(0)$ and $\cos\theta_0 = -1$. Direct estimation of $G^2(t)$ also recovers the optimal initial condition, and the transient oscillation dynamics under such condition are given by

$$G^2(t) = 1 + \frac{2}{\mu - 1}\sin^2 E_1 t. \tag{A6}$$

The results are consistent with Eq. (57) in the main text, where the oscillation period $T = \pi/E_1$ is just the phase-slip period estimated from Eq. (54).

[1] J. Holmboe, On the behavior of symmetric waves in stratified shear layers, Geofys. Publikas. **24**, 67 (1962).

[2] R. A. Cairns, The role of negative energy waves in some instabilities of parallel flows, J. Fluid Mech. **92**, 1 (1979).

[3] A. D. D. Craik, *Wave Interactions and Fluid Flows*, Cambridge Monographs on Mechanics (Cambridge University Press, Cambridge, 1985).

[4] P. G. Baines and H. Mitsudera, On the mechanism of shear flow instabilities, J. Fluid Mech. **276**, 327 (1994).

[5] E. Heifetz, C. H. Bishop, and P. Alpert, Counterpropagating Rossby waves in the barotropic Rayleigh model of shear instability, Q. J. R. Meteorolog. Soc. **125**, 2835 (1999).

[6] E. Heifetz, C. H. Bishop, B. J. Hoskins, and J. Methven, The counterpropagating Rossby-wave perspective on baroclinic

instability. I: Mathematical basis, Q. J. R. Meteorolog. Soc. **130**, 211 (2004).

[7] E. Heifetz and J. Methven, Relating optimal growth to counter-propagating Rossby waves in shear instability, Phys. Fluids **17**, 064107 (2005).

[8] A. Guha and G. Lawrence, A wave interaction approach to studying nonmodal homogeneous and stratified shear instabilities, J. Fluid Mech. **755**, 336 (2014).

[9] A. Guha and F. E. Udwadia, Nonlinear dynamics induced by linear wave interactions in multilayered flows, J. Fluid Mech. **816**, 412 (2017).

[10] J. R. Carpenter, E. W. Tedford, E. Heifetz, and G. A. Lawrence, Instability in stratified shear flow: Review of a physical interpretation based on interacting waves, Appl. Mech. Rev. **64**, 060801 (2011).

[11] E. Heifetz and A. Guha, Normal form of synchronization and resonance between vorticity waves in shear flow instability, Phys. Rev. E **100**, 043105 (2019).

[12] E. Gengel and E. Heifetz, Minimal nonlinear dynamical system for the interaction between vorticity waves and shear flows, Phys. Rev. E **105**, 065109 (2022).

[13] J. D. Crawford and E. Knobloch, Symmetry and symmetry-breaking bifurcations in fluid dynamics, Annu. Rev. Fluid Mech. **23**, 341 (1991).

[14] L. Magri, P. J. Schmid, and J. P. Moeck, Linear flow analysis inspired by mathematical methods from quantum mechanics, Annu. Rev. Fluid Mech. **55**, 541 (2023).

[15] H. Qin, R. Zhang, A. S. Glasser, and J. Xiao, Kelvin-Helmholtz instability is the result of parity-time symmetry breaking, Phys. Plasmas **26**, 032102 (2019).

[16] Y. Fu and H. Qin, The physics of spontaneous parity-time symmetry breaking in the Kelvin-Helmholtz instability, New J. Phys. **22**, 083040 (2020).

[17] T. W. David, P. Delplace, and A. Venaille, How do discrete symmetries shape the stability of geophysical flows? Phys. Fluids **34**, 056605 (2022).

[18] V. Yakubovich and V. Starzhinskii, *Linear Differential Equations with Periodic Coefficients* (Wiley, New York, 1975), Vol. 1.

[19] O. N. Kirillov, *Nonconservative Stability Problems of Modern Physics*, 2nd ed. (De Gruyter, Berlin, 2021).

[20] O. N. Kirillov and D. E. Pelinovsky, *Nonlinear Physical Systems: Spectral Analysis, Stability and Bifurcations* (Wiley, New York, 2014).

[21] R. Zhang, H. Qin, R. C. Davidson, J. Liu, and J. Xiao, On the structure of the two-stream instability-complex G-Hamiltonian structure and Krein collisions between positive- and negative-action modes, Phys. Plasmas **23**, 072111 (2016).

[22] A. Melkani, Degeneracies and symmetry breaking in pseudo-Hermitian matrices, Phys. Rev. Res. **5**, 023035 (2023).

[23] R. Zhang, H. Qin, and J. Xiao, PT-symmetry entails pseudo-Hermiticity regardless of diagonalizability, J. Math. Phys. **61**, 012101 (2020).

[24] C. M. Bender, P. E. Dorey, C. Dunning, A. Fring, D. W. Hook, H. F. Jones, S. Kuzhel, G. Lévai, and R. Tateo, *PT Symmetry: In Quantum and Classical Physics* (World Scientific, Singapore, 2019).

[25] Y. Ashida, Z. Gong, and M. Ueda, Non-Hermitian physics, Adv. Phys. **69**, 249 (2020).

[26] K. Ding, C. Fang, and G. Ma, Non-Hermitian topology and exceptional-point geometries, Nat. Rev. Phys. **4**, 745 (2022).

[27] K. G. Makris, R. El-Ganainy, D. N. Christodoulides, and Z. H. Musslimani, Beam dynamics in $\mathcal{PT}$ symmetric optical lattices, Phys. Rev. Lett. **100**, 103904 (2008).

[28] Q. Zhong, D. N. Christodoulides, M. Khajavikhan, K. G. Makris, and R. El-Ganainy, Power-law scaling of extreme dynamics near higher-order exceptional points, Phys. Rev. A **97**, 020105(R) (2018).

[29] K. G. Makris, Transient growth and dissipative exceptional points, Phys. Rev. E **104**, 054218 (2021).

[30] A. Pikovsky, M. Rosenblum, and J. Kurths, *Synchronization: A Universal Concept in Nonlinear Sciences*, Cambridge Nonlinear Science Series (Cambridge University Press, Cambridge, 2001).

[31] S. H. Strogatz, *Nonlinear Dynamics and Chaos: With Applications to Physics, Biology, Chemistry, and Engineering*, 2nd ed. (CRC Press, Boca Raton, FL, 2015).

[32] B. F. Farrell and P. J. Ioannou, Generalized stability theory. Part I: Autonomous operators, J. Atmos. Sci. **53**, 2025 (1996).

[33] P. J. Schmid, Nonmodal stability theory, Annu. Rev. Fluid Mech. **39**, 129 (2007).

[34] R. Kerswell, Nonlinear nonmodal stability theory, Annu. Rev. Fluid Mech. **50**, 319 (2018).

[35] W. D. Smyth and J. R. Carpenter, *Instability in Geophysical Flows* (Cambridge University Press, Cambridge, 2019).

[36] P. G. Drazin, *Introduction to Hydrodynamic Stability* (Cambridge University Press, Cambridge, 2002).

[37] Z. J. Mao and Z. B. Guo, Coherent structure formation via spatial phase coupling in two-dimensional (potential) vorticity-conserved systems, Phys. Rev. Fluids **7**, 074702 (2022).

[38] E. Heifetz, N. Harnik, and T. Tamarin, Canonical Hamiltonian representation of pseudoenergy in shear flows using counter-propagating Rossby waves, Q. J. R. Meteorolog. Soc. **135**, 2161 (2009).

[39] E. Heifetz and A. Guha, A generalized action-angle representation of wave interaction in stratified shear flows, J. Fluid Mech. **834**, 220 (2018).

[40] R. Kollár and P. D. Miller, Graphical Krein signature theory and Evans-Krein functions, SIAM Rev. **56**, 73 (2014).

[41] H. Qin, Y. Fu, A. S. Glasser, and A. Yahalom, Spontaneous and explicit parity-time-symmetry breaking in drift-wave instabilities, Phys. Rev. E **104**, 015215 (2021).

[42] I. Rotter, A non-Hermitian Hamilton operator and the physics of open quantum systems, J. Phys. A: Math. Theor. **42**, 153001 (2009).

[43] H. Eleuch and I. Rotter, Resonances in open quantum systems, Phys. Rev. A **95**, 022117 (2017).

[44] E. Heifetz, J. Mak, J. Nycander, and O. Umurhan, Interacting vorticity waves as an instability mechanism for magnetohydrodynamic shear instabilities, J. Fluid Mech. **767**, 199 (2015).

[45] Z. B. Guo and P. H. Diamond, From phase locking to phase slips: A mechanism for a quiescent H mode, Phys. Rev. Lett. **114**, 145002 (2015).

[46] Y. Zhang, Z. B. Guo, and P. H. Diamond, Curvature of radial electric field aggravates edge magnetohydrodynamics mode in toroidally confined plasmas, Phys. Rev. Lett. **125**, 255003 (2020).

[47] G. A. Starkov, M. V. Fistul, and I. M. Eremin, Formation of exceptional points in pseudo-Hermitian systems, Phys. Rev. A **108**, 022206 (2023).